HHS Public Access

Author manuscript

J Magn Reson Imaging. Author manuscript; available in PMC 2023 July 07.

Published in final edited form as:

J Magn Reson Imaging. 2022 April ; 55(4): 1060–1081. doi:10.1002/jmri.27744.

Three-Dimensional Printed Anatomic Models Derived From Magnetic Resonance Imaging Data: Current State and Image Acquisition Recommendations for Appropriate Clinical Scenarios

Varsha R. Talanki[1], **Qi Peng, PhD**[1], **Stephanie B. Shamir, MD**[1], **Steven H. Baete, PhD**[2], **Timothy Q. Duong, PhD**[1], **Nicole Wake, PhD**[1,2,*]

[1]Department of Radiology, Montefiore Medical Center, Albert Einstein College of Medicine, Bronx, New York, USA

[2]Center for Advanced Imaging Innovation and Research (CAI[2]R) and Bernard and Irene Schwartz Center for Biomedical Imaging, Department of Radiology, NYU Langone Health, NYU Grossman School of Medicine, New York, New York, USA

Abstract

Three-dimensional (3D) printing technologies have been increasingly utilized in medicine over the past several years and can greatly facilitate surgical planning thereby improving patient outcomes. Although still much less utilized compared to computed tomography (CT), magnetic resonance imaging (MRI) is gaining traction in medical 3D printing. The purpose of this study was two-fold: 1) to determine the prevalence in the existing literature of using MRI to create 3D printed anatomic models for surgical planning and 2) to provide image acquisition recommendations for appropriate clinical scenarios where MRI is the most suitable imaging modality. The workflow for creating 3D printed anatomic models from medical imaging data is complex and involves image segmentation of the regions of interest and conversion of that data into 3D surface meshes, which are compatible with printing technologies. CT is most commonly used to create 3D printed anatomic models due to the high image quality and relative ease of performing image segmentation from CT data. As compared to CT datasets, 3D printing using MRI data offers advantages since it provides exquisite soft tissue contrast needed for accurate organ segmentation and it does not expose patients to unnecessary ionizing radiation. MRI, however, often requires complicated imaging techniques and time-consuming postprocessing procedures to generate high-resolution 3D anatomic models needed for 3D printing. Despite these challenges, 3D modeling and printing from MRI data holds great clinical promises thanks to emerging innovations in both advanced MRI imaging and postprocessing techniques.

In medicine, three-dimensional (3D) printing, also known as additive manufacturing or rapid prototyping, represents the fabrication of physical objects from volumetric medical imaging

*Address reprint requests to: N.W., 111 East 210th Street, Bronx, NY 10467, USA. nwake@montefiore.org.

Evidence Level: 2

Technical Efficatcy: 5

data, with the intent of positively impacting patient care. 3D printing patient-specific anatomical data extend the current capabilities of conventional 3D visualization by allowing radiologists, surgeons, and other physicians to physically hold patient-specific models in their hands and use visuo-haptic inputs to better understand both complex anatomical structures as well as the condition being treated. Recent advances of 3D printing have allowed 3D printing in medicine to gain tremendous momentum and increased utilization of 3D printing demonstrates promising results in preoperative surgical planning.[1–6] In addition, by allowing for improved understanding of anatomy, enabling precontouring of implants, and providing real-time guidance in the operating room (OR), 3D printed anatomic models and guides can reduce OR costs secondary to shortening procedure times and possibly improve patient outcomes.[7–11]

3D printing technology was introduced in the 1980s, and it encompasses various processes intended to generate a physical 3D model from a digital file.[12,13] Clinical applications of 3D printing began with computed tomography (CT) images, with the first digitally manufactured 3D model ever produced from CT imaging created in the early 1980s using a milling process.[14] The use of milling to produce prostheses continued through the 1980s and 1990s with the majority of applications being in craniomaxillofacial surgery.[15,16] In the 1990s, people started to use stereolithography (SLA) to fabricate patient-specific 3D anatomy from CT data, with the advantage of SLA as compared to traditional milling techniques being that the SLA technique does not require a cutting tool.[17] Around that time, there was also a discussion of combining magnetic resonance imaging (MRI) with CT data to get the soft tissue data from MRI and boney reconstructions from CT.[18]

The workflow for creating 3D printed anatomic models from medical imaging data is complex and involves image segmentation of the anatomic regions of interest and conversion of that data into 3D surface meshes, which are compatible with printing technologies. Figure 1 shows a typical workflow for 3D printing from MRI data.

As compared to CT datasets, 3D printing using MRI data offers a few advantages because it provides exquisite soft tissue contrast needed for accurate organ segmentation and it does not expose patients to unnecessary ionizing radiation. MRI datasets, however, are more complex than CT because MRI has a multitude of sequences with acquisition and image-contrast parameters that are challenging to standardize. Consequently, automated image segmentation in MRI often does not work, global threshold masks are not very useful and suitable thresholds for organs with similar signal intensities are often not found. Furthermore, edge detection and region growing techniques often do not work due to the similar signal intensities found in neighboring structures. Accordingly, the segmentation of MRI datasets has become a complex task for clinicians. Manual segmentation must often be performed, but manual segmentation is tedious, time-consuming, and operator dependent. Another challenge is the long printing and design time, typically 3–5 days.[19] The average image post-processing for multipart renal mass models has been reported to be 7 hours each with a printing time of 10 hours.[1] Despite the challenges in 3D segmentation and modeling from MRI data, 3D modeling and printing from MRI data holds clinically important promises if these challenges can be overcome.

Recent innovations and reduced cost have made 3D printing technologies accessible to many hospitals; and over the last several years there been an increase in hospitals utilizing 3D printing at the point of care.[20] However, although many hospitals are currently utilizing 3D printed anatomic models for clinical care, it is unknown how widespread the use of MRI is as the source data for these models. The purpose of this literature review was 1) to determine the prevalence in the existing literature of using MRI to create 3D printed anatomic models for surgical planning and 2) to provide image acquisition recommendations for appropriate clinical scenarios where MRI is the most suitable imaging modality.

Methods

The authors first conducted a systematic literature review to determine the utilization of MRI for the creation of 3D printed models for surgical planning. In order to identify current publications demonstrating the use of MRI data to create 3D printed anatomic models for surgical planning purposes, a detailed electronic search of Ovid-Medline (PubMed) was conducted. The initial search was performed in June 2020. Search terms included the following:

1. “3D printing” AND “magnetic resonance imaging” AND “planning”
2. “3D printing” AND “MRI” AND “planning”
3. “additive manufacturing” AND “magnetic resonance imaging” AND “planning”
4. “additive manufacturing” AND “MRI” AND “planning”
5. “rapid prototyping” AND “magnetic resonance imaging” AND “planning”
6. “rapid prototyping” AND “MRI” AND “planning”

Only studies in English were reviewed. All animal studies, review papers, editorials, technical notes, and studies only using CT imaging for 3D model generation were excluded. Two of the authors independently reviewed the publications. Data were evaluated to determine what clinical indication 3D printing was being used for, how MRI was utilized to create 3D printed anatomic models, and how these 3D printed models were being utilized for surgical planning.

Next, the appropriate use guidelines for medical 3D printing published by the Radiological Society of North America (RSNA) 3D Printing Special Interest Group (SIG) were searched for clinical situations where 3D printing was deemed usually appropriate (scores of 7–9), with data and experience showing an advantage of 3D printed anatomic models as compared to conventional medical imaging.[21–23]

Finally, for each major clinical indication, currently available MRI acquisition parameters and considerations for novel MRI sequences are described in order to help ensure that all pertinent anatomic structures are well visualized in any 3D printed anatomic models derived from MRI data.

Results and Discussion

Our initial electronic search identified 220 articles with 133 articles remaining after duplicates were removed (Fig. 2). Of these 133 articles, four were excluded based on non-English language literature, leaving 129 which were assessed for eligibility. Out of these 129, 51 articles were excluded because they utilized CT data to construct 3D printed models, 30 review papers were excluded, 3 non-human studies were excluded, 3 technical notes were excluded, and one study was excluded since the 3D printed models were utilized for training. In total, 40 articles met the search term guidelines and were ultimately reviewed (Table 1).[1,19,24–60]

The literature collected was mostly produced in the last six years, with eight articles prior to 2015, three in both 2015 and 2016, nine in both 2017 and 2018, five in 2019, and three in 2020.[1,19,32–60] The two most prominent specialties in the literature review were cardiovascular and neurosurgery with 14 studies focusing on cardiovascular models[25,26,28,33–38,41,44,47,52,61] and 10 focusing on neurosurgical models.[24,30,32,39,40,45,46,58–60] The remaining papers included orthopedic surgery,[27,29,49] liver surgery,[31,42,43] complex neuroblastoma cases,[37,51] a case of perianal fistula,[50] urologic surgery;[1,48,51,53,56,57] and women's health including uterine surgery,[19] breast reconstruction,[51] and brachytherapy for gynecological cancer.[53]

In regard to the appropriate use guidelines for medical 3D printing published by the RSNA 3D Printing SIG, the publications with clinical situations where 3D printing was deemed usually appropriate which utilized MRI to generate 3D printed models are included in Table 2.[21–23] The major clinical scenarios are described below with MRI sequence information from the published papers found in our search (if available) as well as recommendations based on expert opinion.

Cardiovascular Surgery

The cardiovascular system has complex structure and geometry, which can be better visualized and understood with 3D modeling. The literature search performed here identified 14 studies (35%) that utilized MRI to create cardiac models (Table 3).[25,26,28,33–38,41,44,47,52,61] Out of these 14 studies, the majority, 10 of the 14 (71.43%) focused on congenital heart disease (CHD).[26,33,34,36,38,41,44,47,52,61] CHD includes various types of defects: aortic stenosis, atrial septal defects, coarctation of the aorta, Ebstein anomaly, patent ductus arteriosus, patent foramen ovale, truncus arteriosus, double outlet right ventricle, transposition of the great arteries, and ventricular septal defects. Since these defects may be complex and difficult to interpret, 3D-printed models may enable better visualization and analysis of the complex cardiac anatomy, optimize surgical planning and reduce surgical times, ultimately resulting in improved patient outcomes.[62]

Planning for congenital heart surgery using 3D printed models derived from cardiac MRI data has proven to be helpful in many ways, such as decreasing mortality, lowering the chances of finding unexpected results in vivo,[47] allowing surgeons to address challenges prior to surgery,[41] and enabling surgeons to make improved decisions regarding the

surgical plan pre-operatively.[38,44] Specifically, 3D printed models of complex cardiovascular pathology and intracardiac lesions can enable surgeons to overcome the shortcomings of conventional planning by allowing improved identification and dimensional analysis of anatomic structures.[26,28,33,34,36,37] Taking planning one step further, 3D printed models of the native Fontan geometry have also been created to validate simulation results and tissue engineer patient-specific vascular grafts to improve the quality of the surgery.[52]

For pediatric patients, MRI is preferred over CT since MRI does not utilize ionizing radiation. Commonly available MRI techniques applicable for the 3D printing of CHD models include noncontrast 3D steady-state free precession (SSFP) imaging and non electrocardiogram (ECG)-gated or ECG-gated contrast-enhanced 3D fast low-angle shot (FLASH) angiography with or without respiratory navigation.[63] These sequences are applicable for adult cardiovascular patients, although CT is generally the modality of choice due to higher spatial resolution and much less motion blurring compared to MR images. Unlike modern cardiac CT where images are always acquired axially with fast 3D acquisition, MRI acquisitions are advantageous since 2D images can be generated along any orientation with high temporal resolution. However, high-resolution 3D cardiac MRI is time consuming and images are susceptible to motion artifacts. Recent technological developments in both MR imaging and image reconstruction have allowed much higher spatiotemporal resolution to be obtained, potentially making their clinical application in 3D printing a much more competitive alternative to CT. For example, novel 3D free-breathing, self-navigated sequences can provide excellent image quality as compared to routine MR sequences, therefore may be better suited for the creation of 3D models (Fig. 3).[64] With more of these new fast motion-insensitive MRI image protocols becoming clinically available, we anticipate MRI will soon gain wider cardiovascular applications in 3D printing.

Neurosurgery

In neurosurgery, intricate and minute anatomical structures are usually encountered, thus it is imperative that surgeons and interventionalists have a comprehensive understanding of the pathology so that normal brain tissue and proper brain function are both preserved. Herein, of the 40 articles, 10 (25%) highlighted neurosurgical applications (Table 4).[24,30,32,39,40,45,46,58–60] The majority of the reports were single cases or small cohort studies with less than 10 patients, with models being used to enhance anatomic understanding and to help refine the surgical procedure.[24,30,39,40,45,46,58–60] The oldest study found in this search, dating back to 1998, utilized MRI data to create a single 3D model of the human ventricular system.[24] A T2-weighted sequence was selected for the 3D modeling due to the high contrast between brain matter and fluid. Such models could be used for pre-operative planning to help the surgeon decide on the optimal surgical approach and could provide real-time intra-operative guidance.

In regard to 3D anatomic modeling for neurosurgical applications, T1-weighted 3D magnetization-prepared rapid acquisition with gradient echo (MP-RAGE) sequences, which provide excellent contrast between gray and white matter, have been utilized and are recommended.[30,32,40] T1-weighted 3D fast spoiled gradient echo (FSPGR) and 3D time-

of-flight MRI sequences may also be used.[46,58] Additionally, quantitative sequences such as diffusion tensor imaging (DTI) or diffusion spectrum imaging (DSI) for fiber tract extrapolation,[40,46,65,66] functional MRI,[30] and contrast-enhanced MRI[58–60] may be utilized to incorporate more details into 3D models and further facilitate surgical planning (Fig. 4).[66]

For neurosurgical applications, recent imaging technological developments, particularly parallel imaging and compressed sensing, have made high-resolution 3D imaging in everyday clinical practice much more feasible.[67–69] Parallel imaging and compressed sensing are particularly advantageous in 3D MRI since much higher combined acceleration factors can be achieved along both phase encode directions in 3D acquisitions without introducing excessive artifacts and noise. Isotropic spatial resolution with a voxel size of 1.0 mm^3 using 3D T1-weighted MP-RAGE at 3Tesla can be obtained in less than 3 minutes with parallel imaging and compressed sensing.[69] In addition, high-resolution 3D fluid attenuated inversion recovery (FLAIR) and 3D T2-weighted sequences (eg, CUBE for GE, Sampling Perfection with Application optimized Contrasts using different flip angle Evolution [SPACE] for Siemens, and Volume Isotropic Turbo spin echo Acquisition [VISTA] for Philips) can be readily acquired within clinically acceptable scan duration (<4 minutes each)[69] and they will gain growing popularity in neurosurgical planning. Moreover, 3D susceptibility-weighted imaging (SWI) is replacing 2D MRI sequences to visualize venous structures and iron, as well as to detect micro-hemorrhages.[70,71] Traditionally, clinical diffusion-weighted images (DWI) are acquired using single-shot echo planar imaging (EPI) sequences, but these images suffer from poor spatial resolution, spatial distortion, and susceptibility artifacts, not fit for modeling for 3D printing. Recent single-shot turbo spin-echo (TSE) and multishot EPI DWI sequences have enabled higher spatial resolution diffusion imaging with much less distortion.[72–74] There is also a trend to use radial k-space acquisition to reduce motion sensitivity, making high-resolution 3D imaging clinically more reliable.[75] As these novel sequences are more widely utilized, more neurosurgical applications for 3D printing using MRI data are expected.

Liver Surgery

For liver surgeries including hepatectomy, liver transplant, and tumor resection procedures, hybrid CT and MRI approaches have been used to distinguish between hepatic arteries, portal veins, bile duct, and tumor in the hepatic hilum.[31,42,43] 3D printed liver models have been shown to facilitate surgery by providing an enhanced understanding of the spatial relationships between vascular and biliary structures and demonstrated identical anatomic and geometrical landmarks in the 3D printed and native livers.[31]

Similar to cardiovascular surgery, MRI is a preferable imaging modality for pediatric liver surgical planning due to ionizing radiation concerns for infants and children. To allow high-resolution 2D or 3D MR imaging of the abdomen, respiratory motion control such as breath-hold, respiratory triggering, respiratory gating, and respiratory navigation is generally needed. Fat suppression is also desirable to improve contrast of lesions and to reduce potential contaminating artifacts. Dixon's method-based sequences (i.e. mDixon for Philips, IDEAL for GE, Dixon for Siemens) have gained wide-spread clinical use. In this technique, multiple echoes with different echo times (TEs) are acquired in each repetition time (TR),

which allows water-only, fat-only, in-phase, and out-of-phase water/fat contrast image sets to be reconstructed during postprocessing.[76] A fast 3D breath-hold Dixon's method-based sequence can also be used in liver MRI for precontrast and postcontrast imaging for tumor or vascular evaluation (Fig. 5).[77] New clinically available MR sequences using radial k-space acquisition[78] with less motion sensitivity can also be combined with Dixon's method to enhance diagnosis reliability or image contrast.[79] These advanced sequences are becoming more widely available on clinical scanners; therefore, it is anticipated that these emerging fast MR sequences with high spatial resolution and less motion blurring will gain more applications for 3D printing in clinical practice, particularly for liver imaging limited by patient motion.

Urologic Surgery

The search conducted here yielded six collected articles related to urologic surgery which focused on models for renal and prostate cancer.[1,48,51,53,56,57] 3D printed renal cancer models have been shown to facilitate surgical planning for robotic assisted partial nephrectomy[1,53,80,81] and Wilms Tumor resection planning.[51] MRI acquisitions used to create 3D printed renal cancer models have included 1.5 Tesla imaging with a 3D postcontrast fat suppressed gradient echo T1-weighted sequence with a spatial resolution of $1.4\ \text{mm} \times 1.4\ \text{mm} \times 2\ \text{mm}$ and a breath-hold ranging from 13 seconds to 20 seconds.[1,82] Arterial, venous, and collecting phase images are utilized for the appropriate visualization of the arterial, venous, and collecting systems, respectively. Although our search did not generate any reports of 3D printed renal cancer models created with MRI sequences based on the 3D Dixon method, as discussed in the "Liver Surgery" section, it is likely these sequences can provide equal or better outcome in kidney imaging, as shown in Fig. 5.

For urologic applications, presurgical 3D printed prostate cancer models derived from MRI data can also be helpful for presurgical planning.[48,82] MR image acquisition can include a 3D volumetric T2-weighted imaging sequence with a spatial resolution of $0.6\ \text{mm} \times 0.6\ \text{mm} \times 1.0\ \text{mm}$ at 3 T; and these T2-weighted anatomic images can be co-registered with DWI or 3D dynamic contrast-enhanced (DCE) images for better lesion characterization.[82] Axial 3D T2-weighted MRI with an imaging slice thickness of 2.5 mm has also been utilized to create patient-specific 3D printed prostate cutting guides; and these have been used to successfully section the prostate for slice-by-slice comparison with histopathological findings.[56]

Figure 6 shows representative 3D printed kidney and prostate cancer models derived from MRI data. 3D printing can be especially helpful in understanding the abnormal anatomy and spatial relationships of pertinent anatomical structures in these cases and can help facilitate organ sparing surgery.[1,53,82]

Orthopedic Surgery

In orthopedic surgery, CT is utilized more often than MRI due to the fact that CT uses X-rays which leads to high contrast between bone and lean tissues. Furthermore, many automated image postprocessing algorithms are already available clinically to segment

anatomical regions of interest such as bone based on the Hounsfield unit scale.[21] Despite this, MRI, which is superior at visualizing soft tissue structures, may be used to examine bones, joints, and soft tissues including cartilage, muscles, and tendons for injuries or the presence of structural abnormalities or other conditions. This review yielded three articles which utilized MRI to create 3D-printed anatomic models for surgical planning for orthopedic procedures.[27,29,49] In two out the three papers, MRI played a supporting role compared to CT.[29,49] In the other article, only MR images were used with better model results desired.[27]

For the combined approach, Punyaratabandhu et al described the creation of models for presurgical planning on extra-compartmental bone tumors with a hybrid CT and MRI approach, since CT is superior at segmenting bones and MRI is better at highlighting soft tissue structures. They found that the models helped to guide the orthopedic surgeon to create personalized pre-operative plans and perform physical simulations, leading to decreased blood loss, operative times, and surgical incision lengths.[49] Next, Bellanova et al utilized a combined CT and MRI approach for surgical planning in four pediatric tibial bone sarcoma resection cases.[29] A multimodal registration algorithm was used to fuse the CT, MRI, and tumor volume which was manually delineated from an MRI series in which the tumor boundaries were well visualized. After preoperative planning, a surgical guide that was fitted to a unique position on the tibia was manufactured using 3D printing. A second instrument was manufactured to adjust the bone allograft to fit the resection gap accurately. The authors found that accurate preoperative localization of the tumor provided allowed resection with adequate but minimal safe margins, and the patient-specific surgical guides improved the accuracy of the resection during the surgery, thus preventing unnecessary resection and preserving, when needed, articular cartilage in young patients.[29] Hung et al used only MRI data and detailed the creation of a 3D printed model for a 5-year-old boy with progressive limping and shortening of the left lower limb following septic arthritis of the ipsilateral joint with the sequelae of avascular necrosis of the femoral head and lateral subluxation of the joint.[27] Due to the patient's young age, MRI was performed in order to limit radiation and a 3D printed model was constructed for pediatric proximal femoral corrective osteotomy. In comparison to CT, the boney boundary on MRI was less defined, so to overcome this challenge, the contour was manually outlined by a technician. Although the MRI model was not as smooth as CT-derived models, it was understood that the model was still beneficial for the surgeons without exposing the patient to radiation.[27]

MRI has traditionally been limited in orthopedic surgery, since MRI is inherently disadvantaged in imaging cortical bone, which has a low proton density and a very low T2 value, leading to dark signal on traditional MRI images. As described above, MRI is often obtained pre-operatively in addition to CT, in order to properly visualize soft tissues along with the bones (Fig. 7). If it was possible to adequately visualize the bone using MRI, then the need for CT could be eliminated, preventing a patient from being exposed to ionizing radiation and reducing costs, ultimately making it highly valuable for any orthopedic or craniomaxillofacial surgeries.[83,84] In addition, this could be beneficial for radiation oncology applications where CT has been traditionally used as the primary imaging modality for clinical treatment planning, in combination with MRI for soft tissue

delineation. Herein, the patient treatment workflow can be greatly improved if only MRI is needed.

The development of MRI sequences which better delineate bone has been a topic of great interest over the last decade. “Black Bone” MRI techniques that do not enhance soft tissues but rather enhance the zones of separation between bones and soft tissues, could be used to differentiate bone from lean tissues. However, this MR technique assumes cortical bone has low signal while all other non-bone within the area contribute to MR signal and is thus susceptible to artifacts arising from air and tissue interfaces. Another major direction of MRI is the application of ultra-short TE (UTE) or zero-TE (ZTE) sequences, emerging imaging techniques that are becoming more clinical available to provide “positive” contrast between bone and lean tissues.[85,86] In both techniques, radial k-space lines are acquired starting from the k-space center to the peripheral areas, leading to effective TE of close to zero (generally less than 100 μsec), much less than the T2 of cortical bone (0.28 msec–0.38 msec).[87,88] To enhance contrast between the short T2 components (eg, cortical bone) and the long T2 tissues (eg, muscles, typically with higher signal than cortical bone), various soft tissue suppression techniques have been developed.[89] UTE/ZTE MRI are gaining more clinical applications in diagnostic imaging such as in bone-related conditions.[90,91] Therefore, “synthetic CT” images, reconstructed from UTE/ZTE MRI images to simulate CT images, have been heavily studied recently.[92,93] Additionally, “synthetic CT” images can be used in hybrid PET/MRI scanners to generate surrogate bone density maps for PET attenuation correction.[94,95] The clinical applications of UTE/ZTE MRI are steadily growing. However, to the best of our knowledge, there are few 3D printing studies or reports based on images obtained from UTE/ZTE MRI sequences.[96,97] We believe that 3D printing and UTE/ZTE MRI have great potential to grow synergistically. For example, a recent study created a 3D-printed phantom mimicking cortical bone to evaluate UTE MRI techniques and we expect more developments such as this in the future.[98]

Other Considerations and Future Perspectives

There has been a significant increase of the use of 3D printing from MRI data over the past 5 years. However, at this time, image acquisition is generally obtained based on established clinical protocols and is not optimized for 3D printing purposes. If a clinician requests a 3D printed model prior to the image acquisition, dedicated MR protocols can be tailored for 3D printing to include the highest possible spatial resolution, spatial fidelity, signal-to-noise ratio (SNR), and contrast-to-noise ratio (CNR) in the region of interest.[21] In order to facilitate the widespread utilization of 3D printing in medicine, it is necessary to establish the global optimization of 3D printing compatible protocols for all patients. Standard diagnostic MR sequences that are also compatible with 3D printing will not only improve patient diagnosis but also will enhance surgical planning and clinical care in a more efficient and cost-effective workflow. Fortunately, we are seeing a trend of more high-resolution 3D MRI protocols being accepted by radiologists in their everyday practice particularly in neurological and musculoskeletal applications, thanks to the recent technological development in rapid MR imaging. Looking ahead, time resolved or motion insensitive radial-based MR data acquisition, UTE/ZTE MRI, more advanced iterative or deep-learning based image reconstruction techniques will become more clinical available,

and will gain widespread adoption for many clinical applications, particularly in high-resolution 3D or 4D imaging, which will allow 3D printed models to be readily created if needed.[99,100]

Although the craniomaxillofacial (CMF) specialty was one of the earliest fields to adopt the use of 3D models derived from medical imaging data[101,102] and the usage of CT data over MRI data to create CMF models for presurgical planning is an accepted practice,[103] our search did not find any articles utilizing MRI for surgical planning of CMF procedures. With the introduction of novel black bone and UTE/ZTE MRI sequences, the use of MRI could become more prevalent in these case types.[96]

Similarly, 3D printing for surgical planning has been used in conjoined twins separation since the 1990s,[104] and although our search did come up with one article that mentioned 3D printing for conjoined twins separation, this article did not actually utilize 3D printing for their own cases but instead just mentioned the use of 3D printing at other institutions for these case types.[105] For conjoined twins separation, combining CT with MRI and utilizing novel MRI sequences as well as incorporating quantitative information such as that from diffusion MRI into the 3D models may provide even extra value for clinicians.[40,66]

In regard to 3D printing technologies commonly used in hospitals, the major types include material extrusion, material jetting, binder jetting, vat photopolymerization, and polymer powder bed fusion (HP Jet Fusion, HP Inc, Palo Alto, CA). Materials currently used to create medical models with these technologies are generally rigid plastics and powders, although a combination of rigid and flexible materials may be printed using material jetting or multiextruder material extrusion technologies. Single component models such as bones can be created easily with material extrusion or vat photopolymerization technologies. For these, over-curing in certain regions or dual-extrusion printing may also allow for dual colored models highlighting certain anatomic regions of interest. Full color printing may be achieved using material jetting, binder jetting, or powder bed fusion. For medical models, color may be necessary to differentiate different structures in anatomic models, which depict multiple pertinent anatomic structures such as a kidney with a lesion, artery, vein, and collecting system. 3D printed anatomic models that are used for simulations should closely mimic human tissue properties, so for these, material jetting with different combinations of rigid and flexible materials is most suitable. 3D-printed molds could also be created and filled with suitable anthropomorphic materials.

Most of the commonly available 3D printing materials are not visible with MRI since these materials must be rich in hydrogen. At this time, new 3D printing materials are being developed and their MRI properties are being evaluated.[106] 3D printed models with MRI-visible properties and known geometries would be extremely useful for quality assurance testing to evaluate the ability of MRI systems to safely produce accurate imaging. Furthermore, patient-specific models that incorporate MRI-visible 3D printed materials could have great impact on surgical planning and guiding MRI-guided percutaneous procedures in the future.[107]

Over the past 5 years, many hospitals throughout the United States have brought 3D printing in-house; however, oftentimes this is driven by self-funding or grant support and costs still remain a major concern for this technology.[20] On July 1, 2019 four Category III Current Procedure Terminology (CPT) codes for 3D printed anatomic models and guides were released.[108] Category III CPT codes were established in 2001 and they are used for data collection for emerging technologies that are not yet mature and do not yet meet the criteria for Category I CPT codes, which are for established medical services that have met the requirements of widespread clinical use and have documented efficacy. In order to demonstrate the widespread use of 3D printing in medicine, in conjunction with the release of the Category III CPT codes, the RSNA and the American College of Radiology (ACR) have established a registry for 3D printing.[109] The data collected through this registry will include information about the source imaging, the model construct and effort, 3D printing techniques and effort, as well as the clinical impact of the models; and data will be used to support an application for full reimbursement for 3D printing anatomic models and guides at the point of care. Based on these efforts, it is expected that 3D printed anatomic models and guides will be deemed clinically necessary for certain complicated procedures and these will become part of common medical and surgical practice. In addition, personalized 3D-printed implants, bioregenerative materials, and living bioprinted tissues and organs are expected to further transform medicine over the next several decades.

Conclusions

3D printing based on MRI data can greatly facilitate surgical planning and thereby improves patient outcomes. Current challenges and opportunities include the need to optimize MRI acquisition protocols, improve image segmentation accuracy, reduce image processing time, reduce 3D printing time, reduce cost, and expand the currently limiting insurance reimbursement. Further demonstration of added value is needed for widespread clinical adoption of 3D printing in medicine.

References

1. Wake N, Rude T, Kang SK, et al. 3D printed renal cancer models derived from MRI data: Application in pre-surgical planning. Abdom Radiol (NY) 2017;42(5):1501–1509. [PubMed: 28062895]
2. Esses SJ, Berman P, Bloom AI, Sosna J. Clinical applications of physical 3D models derived from MDCT data and created by rapid prototyping. AJR Am J Roentgenol 2011;196(6):W683–W688. [PubMed: 21606254]
3. Sodian R, Schmauss D, Markert M, et al. Three-dimensional printing creates models for surgical planning of aortic valve replacement after previous coronary bypass grafting. Ann Thorac Surg 2008;85(6):2105–2108. [PubMed: 18498831]
4. Schmauss D, Schmitz C, Bigdeli AK, et al. Three-dimensional printing of models for preoperative planning and simulation of transcatheter valve replacement. Ann Thorac Surg 2012;93(2):e31–e33. [PubMed: 22269765]
5. Izzo RL, O'Hara RP, Iyer V, Hansen R, Meess KM, Nagesh SVS, Rudin S, Siddiqui AH, Springer M, Ionita CN. 3D printed cardiac phantom for procedural planning of a transcatheter native mitral valve replacement. Proc SPIE Int Soc Opt Eng 2016;9789:978908. 10.1117/12.2216952 [PubMed: 28615797]

6. Ripley B, Kelil T, Cheezum MK, et al. 3D printing based on cardiac CT assists anatomic visualization prior to transcatheter aortic valve replacement. J Cardiovasc Comput Tomogr 2016;10(1):28–36. [PubMed: 26732862]
7. Sieira Gil R, Roig AM, Obispo CA, Morla A, Pages CM, Perez JL. Surgical planning and microvascular reconstruction of the mandible with a fibular flap using computer-aided design, rapid prototype modelling, and precontoured titanium reconstruction plates: A prospective study. Br J Oral Maxillofac Surg 2015;53(1):49–53. [PubMed: 25305795]
8. Hanasono MM, Skoracki RJ. Computer-assisted design and rapid prototype modeling in microvascular mandible reconstruction. Laryngoscope 2013;123(3):597–604. [PubMed: 23007556]
9. Zhang YZ, Chen B, Lu S, et al. Preliminary application of computer-assisted patient-specific acetabular navigational template for total hip arthroplasty in adult single development dysplasia of the hip. Int J Med Robot 2011;7(4):469–474. [PubMed: 22113980]
10. Toto JM, Chang EI, Agag R, Devarajan K, Patel SA, Topham NS. Improved operative efficiency of free fibula flap mandible reconstruction with patient-specific, computer-guided preoperative planning. Head Neck 2015;37(11):1660–1664. [PubMed: 24954814]
11. Ferrara F, Cipriani A, Magarelli N, et al. Implant positioning in TKA: Comparison between conventional and patient-specific instrumentation. Orthopedics 2015;38(4):e271–e280. [PubMed: 25901619]
12. Crump SS. Apparatus and method for creating three-dimensional objects. United States patent US 5121329A 1989 Available from: https://patents.google.com/patent/US5121329
13. ISO/TC261., ASTM_CommitteeF42. ISO/ASTM 52900(en) Additive manufacturing - General principles - Terminology 2018. Accessed on June 27, 2020 https://www.iso.org/obp/ui/#iso:std:iso-astm:52900:dis:ed-2:v1:en
14. Marsh JL. Comprehensive care for craniofacial deformities St. Louis: Mosby; 1985.
15. Toth BA, Ellis DS, Stewart WB. Computer-designed prostheses for orbitocranial reconstruction. Plast Reconstr Surg 1988;81(3):315–322. [PubMed: 3340666]
16. Scholz M, Eufinger H, Wehmoller M, Heuser L, Harders A. CAD/CAM (computer-aided design/computer-aided manufacturing) titanium implants for cranial and craniofacial defect reconstruction. Zentralbl Neurochir 1997;58(3):105–110. [PubMed: 9446459]
17. Mankovich NJ, Cheeseman AM, Stoker NG. The display of three-dimensional anatomy with stereolithographic models. J Digit Imaging 1990;3(3):200–203. [PubMed: 2085555]
18. McGurk M, Amis AA, Potamianos P, Goodger NM. Rapid prototyping techniques for anatomical modelling in medicine. Ann R Coll Surg Engl 1997;79(3):169–174. [PubMed: 9196336]
19. Sayed Aluwee S, Zhou X, Kato H, et al. Evaluation of pre-surgical models for uterine surgery by use of three-dimensional printing and mold casting. Radiol Phys Technol 2017;10(3):279–285. [PubMed: 28405900]
20. Mottart X SP. 3D lab in a hospital environment: 3 key reasons why a professional desktop printer is a great fit. Materialise NV White Paper 2017.
21. Chepelev L, Wake N, AW RJ, et al. Radiological Society of North America (RSNA) 3D Printing Special Interest Group (SIG): Guidelines for medical 3D printing and appropriateness for clinical scenarios. 3D Print Med 2018;4(11):1–38. [PubMed: 29782615]
22. Ballard DH, Wake N, Witowski J, et al. Radiological Society of North America (RSNA) 3D Printing Special Interest Group (SIG) clinical situations for which 3D printing is considered an appropriate representation or extension of data contained in a medical imaging examination: Abdominal, hepatobiliary, and gastrointestinal conditions. 3D Print Med 2020;6(1):13. [PubMed: 32514795]
23. Ali A, Ballard DH, Althobaity W, et al. Clinical situations for which 3D printing is considered an appropriate representation or extension of data contained in a medical imaging examination: Adult cardiac conditions. 3D Print Med 2020;6(1):24. [PubMed: 32965536]
24. Vloeberghs M, Hatfield F, Daemi F, Dickens P. Soft tissue rapid prototyping in neurosurgery. Comput Aided Surg 1998;3(2):95–97. [PubMed: 9784958]
25. Markert M, Weber S, Lueth TC. A beating heart model 3D printed from specific patient data. Conf Proc IEEE Eng Med Biol Soc 2007; 2007:4472–4475.

26. Sodian R, Weber S, Markert M, et al. Stereolithographic models for surgical planning in congenital heart surgery. Ann Thorac Surg 2007; 83(5):1854–1857. [PubMed: 17462413]
27. Hung SS, Lee ZL, Lee MY. Clinical application of rapid prototype model in pediatric proximal femoral corrective osteotomy. Orthopedics 2008;31(1):72. [PubMed: 19292166]
28. Jacobs S, Grunert R, Mohr FW, Falk V. 3D-imaging of cardiac structures using 3D heart models for planning in heart surgery: A preliminary study. Interact Cardiovasc Thorac Surg 2008;7(1):6–9. [PubMed: 17925319]
29. Bellanova L, Paul L, Docquier PL. Surgical guides (patient-specific instruments) for pediatric tibial bone sarcoma resection and allograft reconstruction. Sarcoma 2013;2013:787653. [PubMed: 23533326]
30. Spottiswoode BS, van den Heever DJ, Chang Y, et al. Preoperative three-dimensional model creation of magnetic resonance brain images as a tool to assist neurosurgical planning. Stereotact Funct Neurosurg 2013;91(3):162–169. [PubMed: 23446024]
31. Zein NN, Hanouneh IA, Bishop PD, et al. Three-dimensional print of a liver for preoperative planning in living donor liver transplantation. Liver Transpl 2013;19(12):1304–1310. [PubMed: 23959637]
32. Naftulin JS, Kimchi EY, Cash SS. Streamlined, inexpensive 3D printing of the brain and skull. PLoS One 2015;10(8):e0136198. [PubMed: 26295459]
33. Valverde I, Gomez G, Coserria JF, et al. 3D printed models for planning endovascular stenting in transverse aortic arch hypoplasia. Catheter Cardiovasc Interv 2015;85(6):1006–1012. [PubMed: 25557983]
34. Valverde I, Gomez G, Gonzalez A, et al. Three-dimensional patient-specific cardiac model for surgical planning in Nikaidoh procedure. Cardiol Young 2015;25(4):698–704. [PubMed: 24809416]
35. Al Jabbari O, Abu Saleh WK, Patel AP, Igo SR, Reardon MJ. Use of three-dimensional models to assist in the resection of malignant cardiac tumors. J Card Surg 2016;31(9):581–583. [PubMed: 27455392]
36. Farooqi KM, Gonzalez-Lengua C, Shenoy R, Sanz J, Nguyen K. Use of a three dimensional printed cardiac model to assess suitability for biventricular repair. World J Pediatr Congenit Heart Surg 2016;7(3): 414–416. [PubMed: 27009890]
37. Krauel L, Fenollosa F, Riaza L, et al. Use of 3D prototypes for complex surgical oncologic cases. World J Surg 2016;40(4):889–894. [PubMed: 26541866]
38. Bhatla P, Tretter JT, Ludomirsky A, et al. Utility and scope of rapid prototyping in patients with complex muscular ventricular septal defects or double-outlet right ventricle: Does it alter management decisions? Pediatr Cardiol 2017;38(1):103–114. [PubMed: 27837304]
39. Furdová A, Sramka M, Thurzo A, Furdová A. Early experiences of planning stereotactic radiosurgery using 3D printed models of eyes with uveal melanomas. Clin Ophthalmol 2017;11:267–271. [PubMed: 28203052]
40. Gargiulo P, Árnadóttir Í, Gíslason M, Edmunds K, Ólafsson I. New directions in 3D medical modeling: 3D-printing anatomy and functions in neurosurgical planning. J Healthc Eng 2017;2017:1439643. [PubMed: 29065569]
41. Kappanayil M, Koneti NR, Kannan RR, Kottayil BP, Kumar K. Three-dimensional-printed cardiac prototypes aid surgical decision-making and preoperative planning in selected cases of complex congenital heart diseases: Early experience and proof of concept in a resource-limited environment. Ann Pediatr Cardiol 2017;10(2):117–125. [PubMed: 28566818]
42. Madurska MJ, Poyade M, Eason D, Rea P, Watson AJ. Development of a patient-specific 3D-printed liver model for preoperative planning. Surg Innov 2017;24(2):145–150. [PubMed: 28134003]
43. Oshiro Y, Ohkohchi N. Three-dimensional liver surgery simulation: Computer-assisted surgical planning with three-dimensional simulation software and three-dimensional printing. Tissue Eng Part A 2017; 23(11–12):474–480. [PubMed: 28343411]
44. Valverde I, Gomez-Ciriza G, Hussain T, et al. Three-dimensional printed models for surgical planning of complex congenital heart defects: An international multicentre study. Eur J Cardiothorac Surg 2017;52(6):1139–1148. [PubMed: 28977423]

45. Coelho G, Chaves TMF, Goes AF, Del Massa EC, Moraes O, Yoshida M. Multimaterial 3D printing preoperative planning for frontoethmoidal meningoencephalocele surgery. Childs Nerv Syst 2018;34(4):749–756. [PubMed: 29067504]
46. Lin J, Zhou Z, Guan J, et al. Using three-dimensional printing to create individualized cranial nerve models for skull base tumor surgery. World Neurosurg 2018;120:e142–e152. [PubMed: 30121411]
47. Olejnik P, Juskanic D, Patrovic L, Halaj M. First printed 3D heart model based on cardiac magnetic resonance imaging data in Slovakia. Bratisl Lek Listy 2018;119(12):781–784. [PubMed: 30686018]
48. Porpiglia F, Bertolo R, Checcucci E, et al. Development and validation of 3D printed virtual models for robot-assisted radical prostatectomy and partial nephrectomy: urologists' and patients' perception. World J Urol 2018;36(2):201–207. [PubMed: 29127451]
49. Punyaratabandhu T, Liacouras PC, Pairojboriboon S. Using 3D models in orthopedic oncology: Presenting personalized advantages in surgical planning and intraoperative outcomes. 3D Print Med 2018;4 (1):12. [PubMed: 30649645]
50. Sahnan K, Adegbola SO, Tozer PJ, et al. Innovation in the imaging perianal fistula: A step towards personalised medicine. Therap Adv Gastroenterol 2018;11:1756284818775060.
51. Sánchez-Sánchez Á, Girón-Vallejo Ó, Ruiz-Pruneda R, et al. Three-dimensional printed model and virtual reconstruction: An extra tool for pediatric solid tumors surgery. European J Pediatr Surg Rep 2018; 6(1):e70–e76.
52. Siallagan D, Loke YH, Olivieri L, et al. Virtual surgical planning, flow simulation, and 3-dimensional electrospinning of patient-specific grafts to optimize Fontan hemodynamics. J Thorac Cardiovasc Surg 2018;155(4):1734–1742. [PubMed: 29361303]
53. Wake N, Bjurlin MA, Rostami P, Chandarana H, Huang WC. Three-dimensional printing and augmented reality: Enhanced precision for robotic assisted partial nephrectomy. Urology 2018;116:227–228.
54. Chen K, Feng CJ, Ma H, et al. Preoperative breast volume evaluation of one-stage immediate breast reconstruction using three-dimensional surface imaging and a printed mold. J Chin Med Assoc 2019;82(9): 732–739. [PubMed: 31335631]
55. Laan RC, Nout RA, Dankelman J, van de Berg NJ. MRI-driven design of customised 3D printed gynaecological brachytherapy applicators with curved needle channels. 3D Print Med 2019;5:8. [PubMed: 31098743]
56. Rutkowski DR, Wells SA, Johnson B, et al. Mri-based cancer lesion analysis with 3d printed patient specific prostate cutting guides. Am J Clin Exp Urol 2019;7(4):215–222. [PubMed: 31511828]
57. Wake N, Rosenkrantz AB, Huang R, et al. Patient-specific 3D printed and augmented reality kidney and prostate cancer models: Impact on patient education. 3D Print Med 2019;5(1):4. [PubMed: 30783869]
58. Javan R, Schickel M, Zhao Y, et al. Using 3D-printed mesh-like brain cortex with deep structures for planning intracranial EEG electrode placement. J Digit Imaging 2020;33(2):324–333. [PubMed: 31512018]
59. Lador R, Regev G, Salame K, Khashan M, Lidar Z. Use of 3-dimensional printing technology in complex spine surgeries. World Neurosurg 2020;133:e327–e341. [PubMed: 31520760]
60. Ye X, Wang L, Li K, et al. A three-dimensional color-printed system allowing complete modeling of arteriovenous malformations for surgical simulations. J Clin Neurosci 2020;77:134–141. [PubMed: 32418811]
61. Farooqi KM, Uppu SC, Nguyen K, et al. Application of virtual three-dimensional models for simultaneous visualization of Intracardiac anatomic relationships in double outlet right ventricle. Pediatr Cardiol 2016;37(1):90–98. [PubMed: 26254102]
62. Ryan J, Plasencia J, Richardson R, et al. 3D printing for congenital heart disease: A single site's initial three-yearexperience. 3D Print Med 2018;4(1):10. [PubMed: 30649650]
63. Yoo SJ, Thabit O, Kim EK, et al. 3D printing in medicine of congenital heart diseases. 3D Print Med 2015;2(1):3. [PubMed: 30050975]
64. Wake N, Feng L, Piccini D, et al. Whole heart self-navigated 3D radial MRI for the creation of virtual 3D models in congenital heart disease. J Cardiovasc Magn Reson 2016;18(1):P185.

65. Wedeen VJ, Hagmann P, Tseng WY, Reese TG, Weisskoff RM. Mapping complex tissue architecture with diffusion spectrum magnetic resonance imaging. Magn Reson Med 2005;54(6):1377–1386. [PubMed: 16247738]
66. Wake NB, Lin Y; Boada FE; Sodickson DK Vizualizing white matter fiber tracts of the human brain in augmented reality: Initial experience with the Microsoft HoloLens. Paper presented at: Proc ISMRM2017; Honolulu, HI, USA
67. Lustig M, Donoho D, Pauly JM. Sparse MRI: The application of compressed sensing for rapid MR imaging. Magn Reson Med 2007;58(6): 1182–1195. [PubMed: 17969013]
68. Pruessmann KP, Weiger M, Scheidegger MB, Boesiger P. SENSE: Sensitivity encoding for fast MRI. Magn Reson Med 1999;42(5):952–962. [PubMed: 10542355]
69. Mönch S, Sollmann N, Hock A, Zimmer C, Kirschke JS, Hedderich DM. Magnetic resonance imaging of the brain using compressed sensing – Quality assessment in daily clinical routine. Clin Neuroradiol 2020;30(2):279–286. [PubMed: 31098666]
70. McKinney AM, Sarikaya B, Gustafson C, Truwit CL. Detection of microhemorrhage in posterior reversible encephalopathy syndrome using susceptibility-weighted imaging. AJNR Am J Neuroradiol 2012; 33(5):896–903. [PubMed: 22241378]
71. Halefoglu AM, Yousem DM. Susceptibility weighted imaging: Clinical applications and future directions. World J Radiol 2018;10(4):30–45. [PubMed: 29849962]
72. Wang Y, Ma X, Zhang Z, et al. A comparison of readout segmented EPI and interleaved EPI in high-resolution diffusion weighted imaging. Magn Reson Imaging 2018;47:39–47. [PubMed: 29175470]
73. Gumeler E, Parlak S, Yazici G, Karabulut E, Kiratli H, Oguz KK. Single shot echo planar imaging (ssEPI) vs single shot turbo spin echo (ssTSE) DWI of the orbit in patients with ocular melanoma. Br J Radiol 2021; 94(1118):20200825. [PubMed: 33264035]
74. Porter DA, Heidemann RM. High resolution diffusion-weighted imaging using readout-segmented echo-planar imaging, parallel imaging and a two-dimensional navigator-based reacquisition. Magn Reson Med 2009;62(2):468–475. [PubMed: 19449372]
75. Park JE, Choi YH, Cheon JE, et al. Three-dimensional radial VIBE sequence for contrast-enhanced brain imaging: An alternative for reducing motion artifacts in restless children. AJR Am J Roentgenol 2018;210(4):876–882. [PubMed: 29446683]
76. Bhat V, Velandai S, Belliappa V, Illayraja J, Halli KG, Gopalakrishnan G. Quantification of liver fat with mDIXON magnetic resonance imaging, comparison with the computed tomography and the biopsy. J Clin Diagn Res 2017;11(7):TC06–TC10.
77. Yoon JH, Lee JM, Yu MH, Kim EJ, Han JK, Choi BI. Fat-suppressed, three-dimensional T1-weighted imaging using high-acceleration parallel acquisition and a dual-echo Dixon technique for gadoxetic acid-enhanced liver MRI at 3 T. Acta Radiol 2015;56(12):1454–1462. [PubMed: 25480475]
78. Kaltenbach B, Roman A, Polkowski C, et al. Free-breathing dynamic liver examination using a radial 3D T1-weighted gradient echo sequence with moderate undersampling for patients with limited breath-holding capacity. Eur J Radiol 2017;86:26–32. [PubMed: 28027757]
79. Gruber L, Rainer V, Plaikner M, Kremser C, Jaschke W, Henninger B. CAIPIRINHA-Dixon-TWIST (CDT)-VIBE MR imaging of the liver at 3.0T with gadoxetate disodium: A solution for transient arterial-phase respiratory motion-related artifacts? Eur Radiol 2018;28(5):2013–2021. [PubMed: 29264636]
80. Knoedler M, Feibus AH, Lange A, et al. Individualized physical 3-dimensional kidney tumor models constructed from 3-dimensional printers result in improved trainee anatomic understanding. Urology 2015;85(6):1257–1261. [PubMed: 26099870]
81. Silberstein JL, Maddox MM, Dorsey P, Feibus A, Thomas R, Lee BR. Physical models of renal malignancies using standard cross-sectional imaging and 3-dimensional printers: A pilot study. Urology 2014;84 (2):268–272. [PubMed: 24962843]
82. Wake N, Chandarana H, Huang WC, Taneja SS, Rosenkrantz AB. Application of anatomically accurate, patient-specific 3D printed models from MRI data in urological oncology. Clin Radiol 2016;71(6): 610–614. [PubMed: 26983650]

83. Eley KA, Watt-Smith SR, Golding SJ. “black bone” MRI: A novel imaging technique for 3D printing. Dentomaxillofac Radiol 2017;46(3): 20160407. [PubMed: 28128636]
84. Kralik SF, Supakul N, Wu IC, et al. Black bone MRI with 3D reconstruction for the detection of skull fractures in children with suspected abusive head trauma. Neuroradiology 2019;61(1):81–87. [PubMed: 30406272]
85. Robson MD, Gatehouse PD, Bydder M, Bydder GM. Magnetic resonance: An introduction to ultrashort TE (UTE) imaging. J Comput Assist Tomogr 2003;27(6):825–846. [PubMed: 14600447]
86. Weiger M, Pruessmann KP, Hennel F. MRI with zero echo time: Hard versus sweep pulse excitation. Magn Reson Med 2011;66(2):379–389. [PubMed: 21381099]
87. Ma YJ, Zhu Y, Lu X, Carl M, Chang EY, Du J. Short T2 imaging using a 3D double adiabatic inversion recovery prepared ultrashort echo time cones (3D DIR-UTE-cones) sequence. Magn Reson Med 2018;79(5): 2555–2563. [PubMed: 28913879]
88. Ma YJ, Jerban S, Jang H, Chang D, Chang EY, Du J. Quantitative Ultrashort Echo time (UTE) magnetic resonance imaging of bone: An update. Front Endocrinol (Lausanne) 2020;11:567417. [PubMed: 33071975]
89. Li C, Magland JF, Rad HS, Song HK, Wehrli FW. Comparison of optimized soft-tissue suppression schemes for ultrashort echo time MRI. Magn Reson Med 2012;68(3):680–689. [PubMed: 22161636]
90. Ma YJ, West J, Nazaran A, et al. Feasibility of using an inversion-recovery ultrashort echo time (UTE) sequence for quantification of glenoid bone loss. Skeletal Radiol 2018;47(7):973–980. [PubMed: 29396694]
91. Sollmann N, Löffler MT, Kronthaler S, Böhm C, Dieckmeyer M, Ruschke S, Kirschke JS, Carballido-Gamio J, Karampinos DC, Krug R, Baum T. MRI-based quantitative osteoporosis imaging at the spine and femur. J Magn Reson Imaging 2020. 10.1002/jmri.27260.
92. Johnstone E, Wyatt JJ, Henry AM, et al. Systematic review of synthetic computed tomography generation methodologies for use in magnetic resonance imaging-only radiation therapy. Int J Radiat Oncol Biol Phys 2018;100(1):199–217. [PubMed: 29254773]
93. Owrangi AM, Greer PB, Glide-Hurst CK. MRI-only treatment planning: Benefits and challenges. Phys Med Biol 2018;63(5):05TR01.
94. Boss A, Weiger M, Wiesinger F. Future image acquisition trends for PET/MRI. Semin Nucl Med 2015;45(3):201–211. [PubMed: 25841275]
95. Su KH, Friel HT, Kuo JW, et al. UTE-mDixon-based thorax synthetic CT generation. Med Phys 2019;46(8):3520–3531. [PubMed: 31063248]
96. Lu A, Gorny KR, Ho ML. Zero TE MRI for craniofacial bone imaging. AJNR Am J Neuroradiol 2019;40(9):1562–1566. [PubMed: 31467238]
97. van Eijnatten M, Rijkhorst EJ, Hofman M, Forouzanfar T, Wolff J. The accuracy of ultrashort echo time MRI sequences for medical additive manufacturing. Dentomaxillofac Radiol 2016;45(5):20150424. [PubMed: 26943179]
98. Rai R, Manton D, Jameson MG, et al. 3D printed phantoms mimicking cortical bone for the assessment of ultrashort echo time magnetic resonance imaging. Med Phys 2018;45(2):758–766. [PubMed: 29237232]
99. Hyun CM, Kim HP, Lee SM, Lee S, Seo JK. Deep learning for undersampled MRI reconstruction. Phys Med Biol 2018;63(13):135007. [PubMed: 29787383]
100. Hollingsworth KG. Reducing acquisition time in clinical MRI by data undersampling and compressed sensing reconstruction. Phys Med Biol 2015;60(21):R297–R322. [PubMed: 26448064]
101. Marsh JL, Vannier MW. The “third” dimension in craniofacial surgery. Plast Reconstr Surg 1983;71(6):759–767. [PubMed: 6687945]
102. Vannier MW, Marsh JL, Warren JO. Three dimensional CT reconstruction images for craniofacial surgical planning and evaluation. Radiology 1984;150(1):179–184. [PubMed: 6689758]
103. D’Urso PS, Barker TM, Earwaker WJ, et al. Stereolithographic biomodelling in cranio-maxillofacial surgery: A prospective trial. J Craniomaxillofac Surg 1999;27(1):30–37. [PubMed: 10188125]

104. Doski JJ, Heiman HS, Solenberger RI, et al. Successful separation of ischiopagus tripus conjoined twins with comparative analysis of methods for abdominal wall closure and use of the tripus limb. J Pediatr Surg 1997;32(12):1761–1766. [PubMed: 9434022]

105. Mathew RP, Francis S, Basti RS, et al. Conjoined twins - role of imaging and recent advances. J Ultrason 2017;17(71):259–266. [PubMed: 29375901]

106. Mitsouras D, Lee TC, Liacouras P, et al. Three-dimensional printing of MRI-visible phantoms and MR image-guided therapy simulation. Magn Reson Med 2017;77(2):613–622. [PubMed: 26864335]

107. Guenette JP, Himes N, Giannopoulos AA, Kelil T, Mitsouras D, Lee TC. Computer-based vertebral tumor Cryoablation planning and procedure simulation involving two cases using MRI-visible 3D printing and advanced visualization. AJR Am J Roentgenol 2016;207(5): 1128–1131. [PubMed: 27505064]

108. MLN_Matters. July 2019 Update of the Hospital Outpatient Prospective Payment System (OPPS). 2019; MLN Matters Number: MM11318 Available from: https://www.cms.gov/Outreach-and-Education/Medicare-Learning-Network-MLN/MLNMattersArticles/downloads/MM11318.pdf. Accessed August 25, 2020.

109. Radiologic Society of North America and American College of Radiology. 3D Printing Registry 2020; https://nrdr.acr.org/Portal/3DP Accessed August 2\5, 2020.

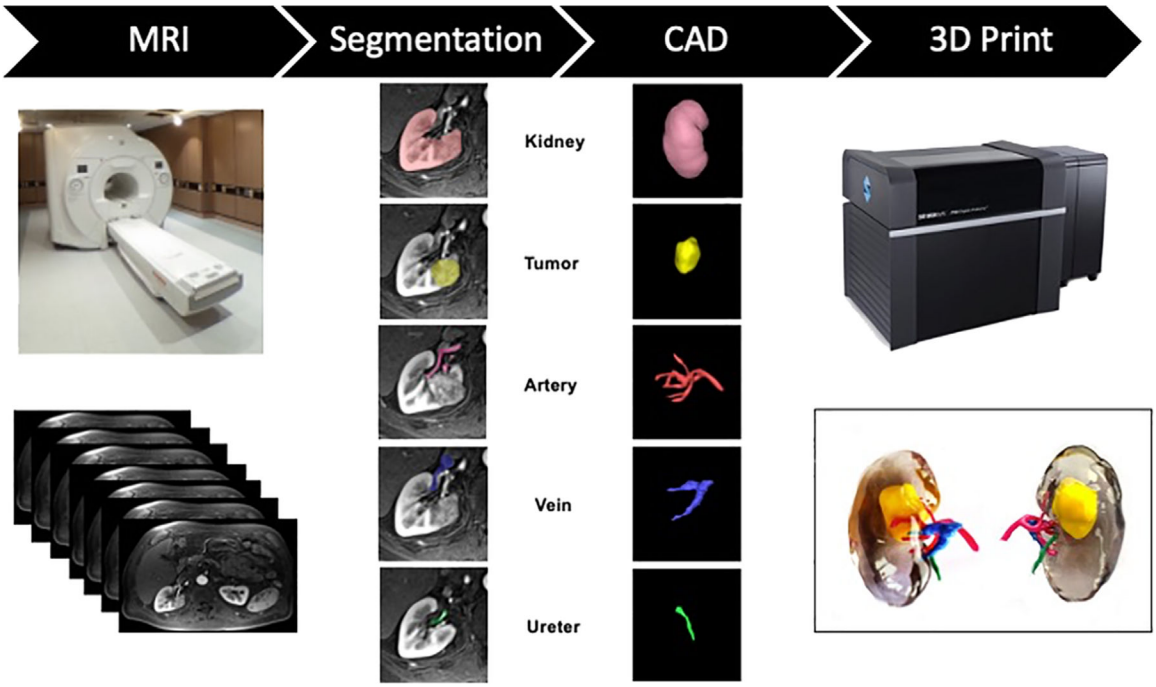

FIGURE 1:
General workflow for 3D printing from a MRI dataset including 1) MRI Exam (Image Acquisition) showing a photograph of a MRI scanner (GE, Waukesha, WI) and axial abdominal images, 2) Image segmentation for a renal cancer model including the kidney, tumor, artery, vein, and ureter, 3) CAD (computer-aided design) modeling of the kidney structures, and 4) 3D printing showing a photography of the J750 Digital Anatomy Printer (Stratasys, Eden Prairie, MN) and anterior and posterior views of the 3D-printed kidney tumor model printed with vero clear, yellow, green, pink, and blue photopolymer materials (Stratasys, Eden Prairie, MN).

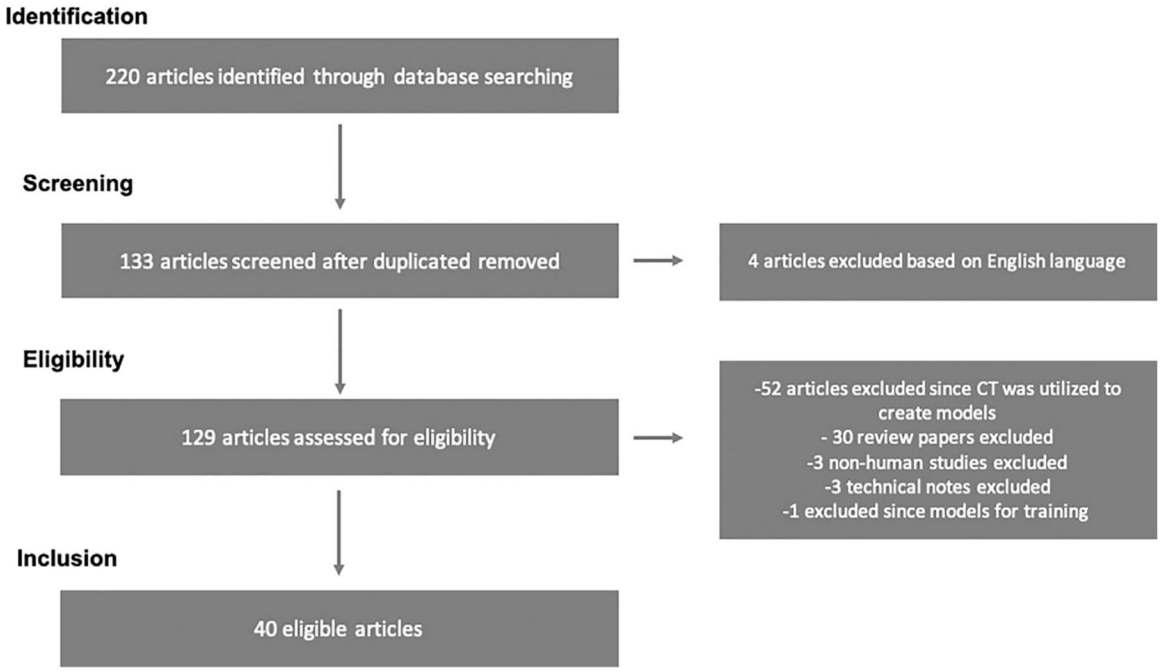

FIGURE 2:
Prisma flow diagram of study selection.

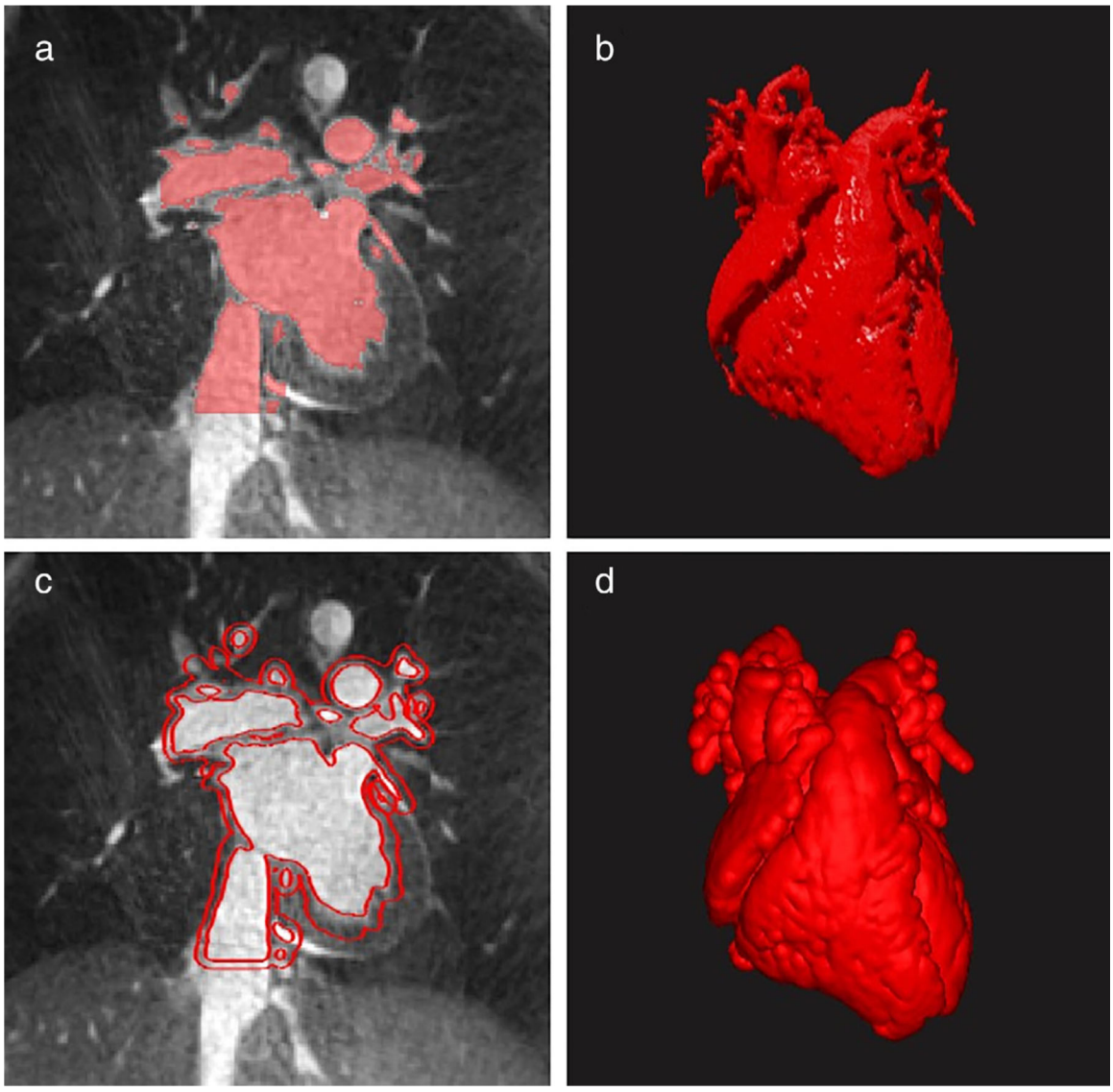

FIGURE 3:

3D cardiovascular segmentation and modeling (D2P, 3D Systems, Rock Hill, SC). (a) Blood pool segmentation using a 3D radial, nonslice-selective, T2-prepared, fat-saturated bSSFP sequence on a 1.5 Tesla MRI scanner (MAGNETOM Aera, Siemens, Erlangen, Germany). The acquisition window (~50 msec–55 msec) was placed in mid-diastole. Imaging parameters were as follows: TR/TE = 3.1/1.56 msec, FOV = 200 mm^3, voxel size = 1 mm^3, FA = 115°, and acquisition time ~5 minutes (~12,000 radial lines). (b) 3D representation of blood pool segmentation. (c) Outline of a 3 mm shell, which was created around the blood pool and would be used for 3D printing shown on the same image as part A. (d) 3D heart model with shell surrounding the hollowed blood pool.

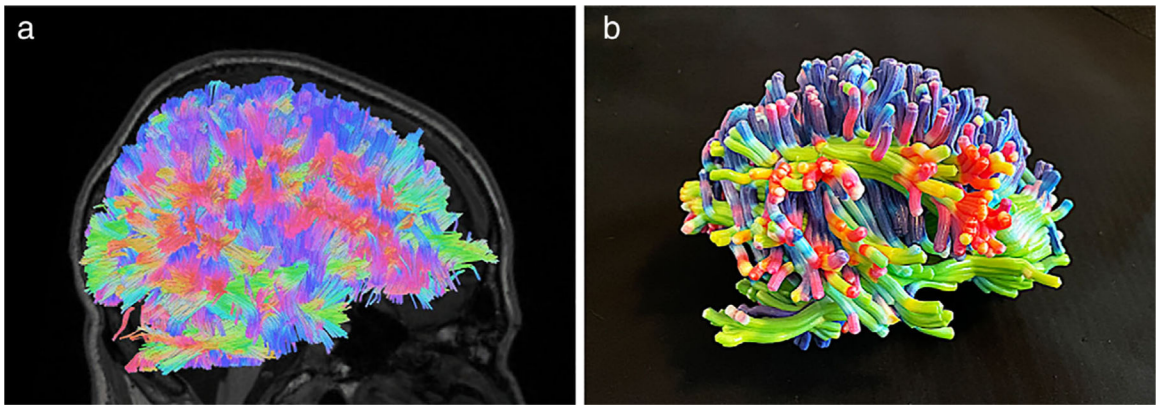

FIGURE 4:

(a) Fiber tracts in a healthy brain generated with a modified streamline tracking algorithm as implemented in DSI Studio (http://dsi-studio.labsolver.org) from DSI obtained on a clinical 3Tesla scanner (Skyra, Siemens, Erlangen, Germany) with a 32-channel head coil using a radially symmetric q-space sampling scheme. (b) 3D printed model of the fiber tracts from part (a) printed using material jetting technology (J750, Stratasys, Eden Prairie, MN) with a 3 mm fiber tract thickness to ensure model fidelity.

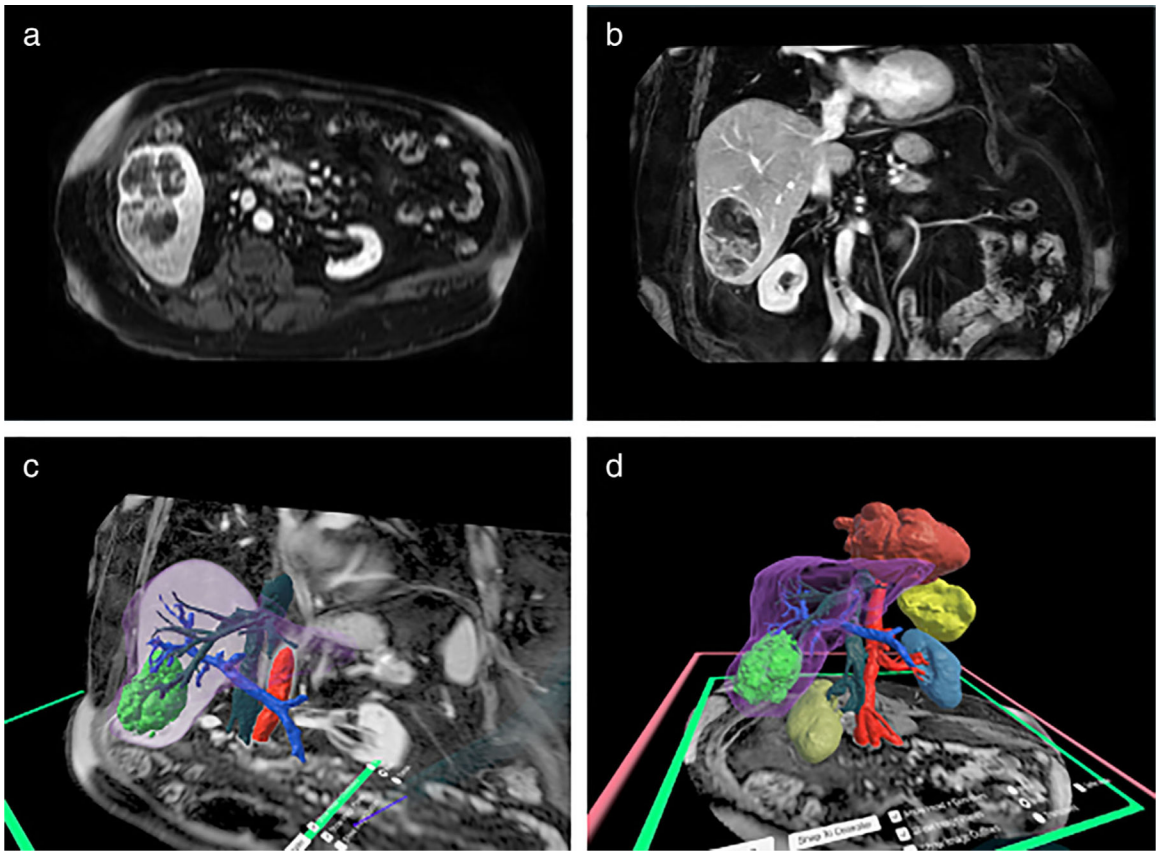

FIGURE 5:

(a) Axial and (b) coronal clinical liver MR images for a patient with hepatocellular carcinoma (HCC) obtained on a 1.5 Tesla scanner using a 3D mDixon breath-hold sequence. (c and d) Virtual Reality (VR) 3D reconstructions with the liver—purple, hepatocellular carcinoma—bright green, hepatic veins—dark green, portal vein—royal blue, aorta—red, right kidney—dark yellow, left kidney—mid blue, spleen—yellow, and heart—dark red shown in the Elucis platform (Realize Medical, Ottawa, Canada). 3D structures can be exported directly from VR for 3D printing.

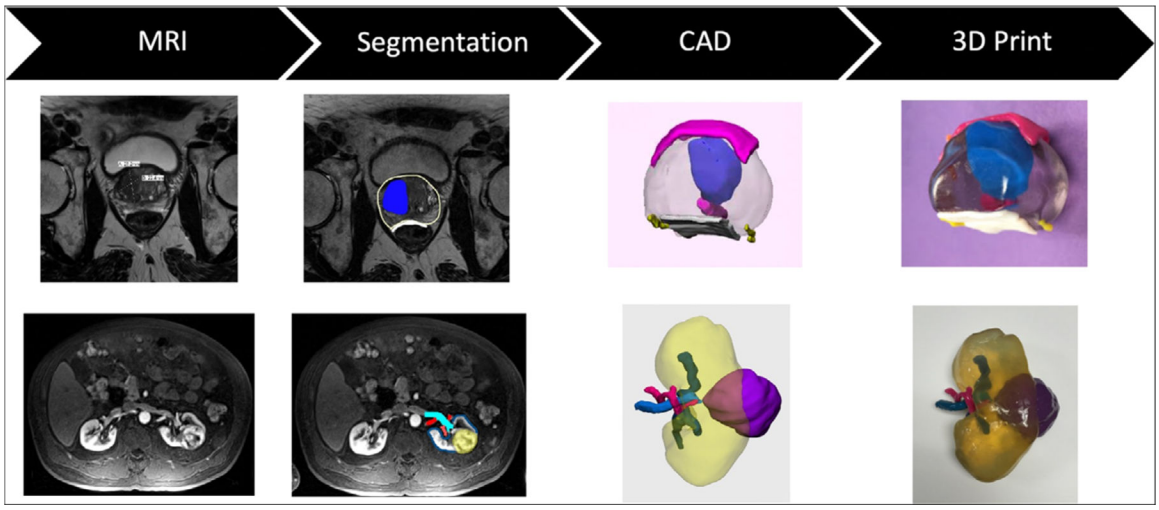

FIGURE 6:

(Top Row) A 68-year-old male with a Prostate Imaging Reporting and Data System (PI-RADS) 5 lesion broadly abutting capsule without gross extraprostatic extension. In this case, the 3D printed model which included the prostate (clear), lesion (blue), bladder neck and urethra (pink), rectal wall (white), and neurovascular bundles (yellow) helped to facilitate a nerve sparing prostatectomy. (Bottom Row) A patient with a 4.4×4.5 cm interpolar renal mass which abuts a lower pole calyx. The 3D printed model which included the kidney (transparent), mass (purple), artery (pink), vein (light blue), and collecting system (dark blue) allowed the vasculature to be well-visualized and facilitated a nephron sparing partial nephrectomy. For both cases, image segmentation and CAD modeling were performed in Mimics and 3-matic (Materialise, Leuven, Belgium) and 3D printing was performed using material jetting technology (J750 and Connex500, Stratasys, Eden Prairie, MN).

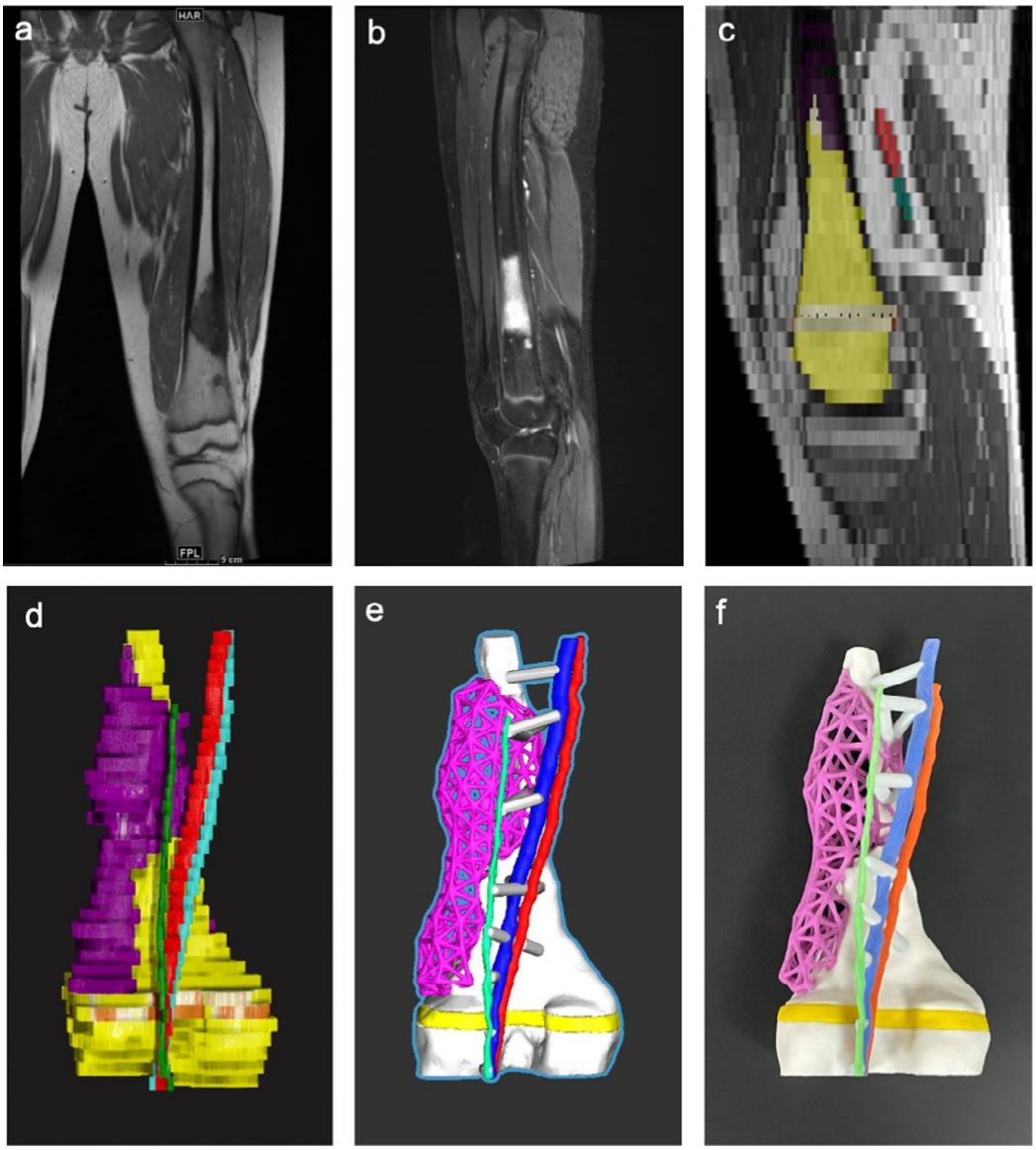

FIGURE 7:

An example of a 3D printed orthopedic model created from MRI data (distal femur with growth plate, tumor, artery, vein, and nerve). (a) Coronal T1-Weighted sequence–TR = 600 msec, TE = 9.4 msec, Slice Spacing = 6 mm, Pixel spacing = 0.714 mm. (b) Sagittal Short TI Inversion Recovery – TR = 3480 msec, TE = 27 msec, ST 6, Slice spacing = 6 mm, Pixel spacing = 0.714 mm. (c) Sagittal slice showing image segmentation using axial images as source data. (d) 3D reconstruction of image segmentation with the bone—yellow, lesion—purple, artery—red, vein—cyan, nerve—green, growth plate—orange. Note the lego-like appearance of the bone due to the poor spatial resolution. (e) Computer-aided design model with the bone-white (shown with significant smoothing to reduce the lego-like appearance), lesion – purple lattice (created in Freeform Plus, 3D Systems, Rock Hill, SC), artery—red, vein—cyan, nerve—green, growth plate—yellow, and struts—gray, which were created to hold vasculature to model. (f) Multicolor 3D printed model printed with binder jetting

technology (CJP 660, 3D Systems, Rock Hill, SC) with the same color scheme as shown in the CAD model.

TABLE 1.

Summary of All Articles Included From the Literature Search Which Reported on the Use of MRI to Create 3D Printed Anatomic Models for Surgical Planning

First Author	Title	Publication Year	DOI	Anatomic Category
Vloeberghs M	Soft tissue rapid prototyping in neurosurgery	1998	10.1002/(SICI)1097–0150(1998)3:4<202::AID-IGS11>3.0.CO;2-F	Neurosurgery
Markert M	A beating heart model 3D printed from specific patient data	2007	10.1109/IEMBS.2007.4353332	Cardiovascular Surgery
Sodian R	Stereolithographic models for surgical planning in congenital heart surgery	2007	10.1016/j.athoracsur.2006.12.004	Cardiovascular Surgery
Hung SS	Clinical application of rapid prototype model in pediatric proximal femoral corrective osteotomy	2008	10.3928/01477447–20080101-19	Orthopedic Surgery
Jacobs S	3D-Imaging of cardiac structures using 3D heart models for planning in heart surgery: a preliminary study	2008	10.1510/icvts.2007.156588	Cardiovascular Surgery
Bellanova L	Surgical guides (patient-specific instruments) for pediatric tibial bone sarcoma resection and allograft reconstruction	2013	10.1155/2013/787653	Orthopedic Surgery
Spottiswoode BS	Preoperative three-dimensional model creation of magnetic resonance brain images as a tool to assist neurosurgical planning	2013	10.1159/000345264	Neurosurgery
Zein NN	Three-dimensional print of a liver for preoperative planning in living donor liver transplantation	2013	10.1002/lt.23729	Liver Surgery
Naftulin JS	Streamlined, Inexpensive 3D Printing of the Brain and Skull	2015	10.1371/journal.pone.0136198	Neurosurgery
Valverde I	Three-dimensional patient-specific cardiac model for surgical planning in Nikaidoh procedure	2015	10.1017/S1047951114000742	Cardiovascular Surgery
Valverde I	3D printed models for planning endovascular stenting in transverse aortic arch hypoplasia	2015	10.1002/ccd.25810	Cardiovascular Surgery
Al Jabbari O	Use of three-dimensional models to assist in the resection of malignant cardiac tumors	2016	10.1111/jocs.12812	Cardiovascular Surgery
Farooqi KM	Application of Virtual Three-Dimensional Models for Simultaneous Visualization of Intracardiac Anatomic Relationships in Double Outlet Right Ventricle	2016	10.1007/s00246–015-1244-z	Cardiovascular Surgery
Farooqi KM	Use of a Three Dimensional Printed Cardiac Model to Assess Suitability for Biventricular Repair	2016	10.1177/2150135115610285	Cardiovascular Surgery
Krauel L	Use of 3D Prototypes for Complex Oncological Cases	2016	10.1007/s00268–015-3295-y	Complex Neuroblastoma
Bhatla P	Utility and Scope of Rapid Prototyping in Patients with Complex Muscular Ventricular Septal Defects or Double-Outlet Right Ventricle: Does it Alter Management Decisions?	2017	10.1007/s00246–016-1489–1	Cardiovascular
Furdova A	Early experiences of planning stereotactic radiosurgery using 3D printed models of eyes with uveal melanomas	2017	10.2147/OPTH.S123640	Neurosurgery

First Author	Title	Publication Year	DOI	Anatomic Category
Gargiulo P	New directions in 3D medical modeling: 3D-printing anatomy and functions in neurosurgical planning	2017	10.1155/2017/1439643	Neurosurgery
Kappanayil M	Three-dimensional-printed cardiac prototypes aid surgical decision-making and preoperative planning in selected cases of complex congenital heart diseases: Early experience and proof of concept in a resource-limited environment	2017	10.4103/apc.APC_149_16	Cardiovascular Surgery
Madurska MJ	Development of a patient-specific 3D-printed liver model for preoperative planning	2014	10.1177/1553350616689414	Liver Surgery
Oshiro Y	Three-dimensional liver surgery simulation: Computer-assisted surgical planning with three-dimensional simulation software and three-dimensional printing	2017	10.1089/ten.TEA.2016.0528	Liver Surgery
Sayed Aluwee SA	Evaluation of pre-surgical models for uterine surgery by use of three-dimensional printing and mold casting	2017	10.1007/s12194–017-0397–2	Women's Health
Valverde I	Three-dimensional printed models for surgical planning of complex congenital heart defects: An international multicentre study	2017	10.1093/ejcts/ezx208	Cardiovascular Surgery
Wake N	3D printed renal cancer models derived from MRI data: Application in pre-surgical planning	2017	10.1007/s00261–016-1022–2	Urologic Surgery
Coelho G	Multimaterial 3D printing preoperative planning for frontoethmoidal meningoencephalocele surgery	2018	10.1007/s00381–017-3616–6	Neurosurgery
Lin J	Using three-dimensional printing to create individualized cranial nerve models for skull base tumor surgery	2018	10.1016/j.wneu.2018.07.236	Neurosurgery
Olejnik P	First printed 3D heart model based on cardiac magnetic resonance imaging data in Slovakia	2018	10.4149/BLL_2018_142	Cardiovascular Surgery
Porpiglia F	Development and validation of 3D printed virtual models for robot-assisted radical prostatectomy and partial nephrectomy: Urologists' and patients' perception	2018	10.1007/s00345–017-2126–1	Urologic Surgery
Punyaratabandhu T	Using 3D models in orthopedic oncology: Presenting personalized advantages in surgical planning and intraoperative outcomes	2018	10.1186/s41205–018-0035–6	Orthopedic Surgery
Sahnan K	Innovation in the imaging perianal fistula: A step towards personalised medicine	2018	10.1177/1756284818775060	Perianal Fistula
Sanchez-Sanchez	Three-dimensional printed model and virtual reconstruction: An extra tool for pediatric solid tumors surgery	2018	10.1055/s-0038–1672165	Complex Neuroblastoma
Siallagan D	Virtual surgical planning, flow simulation, and 3-dimensional electrospinning of patient-specific grafts to optimize Fontan hemodynamics	2018	10.1016/j.jtcvs.2017.11.068	Cardiovascular Surgery
Wake N	Three-dimensional printing and augmented reality: Enhanced precision for robotic assisted partial nephrectomy	2018	10.1016/j.urology.2017.12.038	Urologic Surgery
Chen K	Preoperative breast volume evaluation of one-stage immediate breast reconstruction using three-dimensional surface imaging and a printed mold	2019	10.1097/JCMA.0000000000000155	Women's Health
Laan RC	MRI-driven design of customised 3D printed gynaecological brachytherapy applicators with curved needle channels	2019	10.1186/s41205–019-0047-x	Women's Health
Rutkowski DR	Mri-based cancer lesion analysis with 3d printed patient specific prostate cutting guides	2019	N/A	Urologic Surgery
Wake N	Patient-specific 3D printed and augmented reality kidney and prostate cancer models: impact on patient education	2019	10.1186/s41205–019-0041–3	Urologic Surgery

First Author	Title	Publication Year	DOI	Anatomic Category
Javan R	Using 3D-printed mesh-like brain cortex with deep structures for planning intracranial EEG electrode placement	2020	10.1007/s10278–019-00275–3	Neurosurgery
Lador R	Use of 3-dimensional printing technology in complex spine surgeries	2020	10.1016/j.wneu.2019.09.002	Neurosurgery
Ye X	A three-dimensional color-printed system allowing complete modeling of arteriovenous malformations for surgical simulations	2020	10.1016/j.jocn.2020.04.123	Neurosurgery

TABLE 2.

Clinical Scenarios Where 3D Printing Has Been Deemed Appropriate.[21–23]

Scenario	Rating
Congenital heart disease	
Double outlet right ventricle	9
Double outlet left ventricle	9
Truncus arteriosis	9
Partial anomalous pulmonary venous connection	8
Total anomalous pulmonary venous connection	8
Congenitally corrected transposition of the great arteries	7
Double inlet left ventricle	7
Double inlet right ventricle	7
Tetralogy of fallot, with major aortopulmonary collateral arteries	7
Transposition of the great arteries	7
Unbalanced AV canal	7
Vascular	
Vascular malformations, interventional considerations, slings	8
Design of patient-specific aortic stents	7
Adult cardiac	
Left atrial appendage occlusion	9
Hypertrophic cardiomyopathy	9
Transcatheter aortic valve replacement	9
Transcatheter mitral valve replacement	9
Coronary artery disease and myocardial infarction	7
Cardiac transplant	7
Cardiac tumors	7
Left ventricular assist device	7
Pulmonary valve repair/replacement	7
Postinfarct ventricular septal defect	7
Surgical mitral valve replacement	7
Tricuspid valve repair/replacement	7

Scenario	Rating
Genitourinary	
Renal cancer	9
Prostate cancer	8
Pediatric retroperitoneal genitourinary tumors	7
Urolithiasis, surgical management	7
Hepatobiliary	
Intrahepatic masses, surgical management	8
Musculoskeletal	
Acetabular fracture (complex)	8
Bone/soft tissue neoplasm, with joint and neurovascular involvement	8
Fracture malunion	7
Scoliosis, secondary to congenital vertebral anomaly	7
Craniomaxillofacial	
Congenital malformations of skull and facial bones (complex)	9
Dentofacial anomalies including malocclusion (complex)	9
Malignant neoplasms, bone (complex)	9
Temporomandibular joint disorders (complex)	9
Benign neoplasms, bone (complex)	8
Ear malformations (complex)	8
Facial fractures (complex)	8
Malignant neoplasms, soft tissue (complex)	8
Mandibular fractures (complex)	8
Other diseases of jaw (complex)	8
Cleft lip and palate (complex)	7
Dentofacial anomalies including malocclusion (simple)	7
Malignant neoplasms, bone (simple)	7
Osteochondroplasias (complex)	7
Skull fractures (complex)	7

TABLE 3.

Summary of Articles Which Were Used for Surgical Planning for Cardiovascular Surgeries

Authors	Title	Publication Year	*n*	Case Types	Processing Software	Printing Technology
Markert et al	A beating heart model 3D printed from specific patient data	2007	1	1: Left abnormal subclavian artery connected to the right descending aorta	MeVisLab-Environment (MeVis Research, Bremen, Germany)	Binder Jetting
Sodian et al	Stereolithographic models for surgical planning in congenital heart surgery	2007	2	1: Left abnormal subclavian artey and right descending aorta; 2: Subpulmonary VSD	-	Binder Jetting
Jacobs et al	3D-Imaging of cardiac structures using 3D heart models for planning in heart surgery: a preliminary study	2008	3	1: Malignant Tumor; 2 and 3: Ventricular aneurysms	Mimics 9.0 (Materialise, Leuven, Belgium)	Binder Jetting
Valverde et al	Three-dimensional patient-specific cardiac model for surgical planning in Nikaidoh procedure	2015	1	1: Tansposition of the grat arteries, VSD, and pulmonary stenosis	AYRA (Ikiria, Spain)	Material Extrusion
Valverde et al	3D printed models for planning endovascular stenting in transverse aortic arch hypoplasia	2015	1	1: Hypoplastic aortic arch	AYRA (Ikiria, Spain)	Material Extrusion
Al Jabbari et al	Use of three-dimensional models to assist in the resection of malignant cardiac tumors	2016	2	1: Left atrium osteosarcoma. 2: Encapsulated mass in right atrium extending into the inferior vena cava	Mimics Innovation Suite (Materialise, Leuven, Belgium)	Material Extrusion
Farooqi et al	Application of virtual three-dimensional models for simultaneous visualization of intracardiac anatomic relationships in double outlet right ventricle	2016	6	1–6: DORV	Mimics and 3-matic (Materialise, Leuven, Belgium), Meshlab	N/A
Farooqi et al	Use of a three dimensional printed cardiac model to assess suitability for biventricular repair	2016	1	1: DORV	N/A	Material Jetting
Krauel et al	Use of 3D prototypes for complex surgical oncologic cases	2016	3	1: Right mediastinal mass with invasion of superior vena cava and right atrium, 2–3: Noncardiac cases	VRMed DICOM Platform (ViRVIG research, UPC University, Girona, Spain)	Binder Jetting
Bhatla et al	Utility and scope of rapid prototyping in patients with complex muscular ventricular septal defects or double-outlet right ventricle: Does it alter management decisions?	2017	6	1–3: Complex muscular VSD; 4–6: DORV	Mimics Innovation Suite (Materialise, Leuven, Belgium)	Material Jetting
Kappanayil et al	Three-dimensional printed cardiac prototypes aid surgical decision-making and preoperative planning in selected cases of complex congenital heart diseases: Early experience and proof of concept in a resource-limited environment	2017	5	1–2: DORV, 3–4: Criss-cross atrioventricular connections, 5: transposition of the great arteries with pulmonary atresia	Mimics Innovation Suite (Materialise, Leuven, Belgium)	Powder bed fusion, material jetting, binder jetting, vat photopolymerization
Valverde et al	Three-dimensional printed models for surgical planning of complex congenital heart defects: an international multicentre study	2017	40	1–19: DORV, 20–25: Complex transposition of the great arteries, 26–29: univentricular heart, 30–34: large VSD, 35–37: criss-cross heart, 38: left ventricular outflow tract obstruction, 39: heterotaxy syndrome, 40 discordant	ITK snap (Upenn and UNC), Meshmixer (Autodesk Inc, San Rafael, CA)	Material Extrusion

Authors	Title	Publication Year	*n*	Case Types	Processing Software	Printing Technology
				atrioventricular and ventriculo-arterial connections		
Olejnik et al	First printed 3D heart model based on cardiac magnetic resonance imaging data in Slovakia	2018	1	1: Tetralogy of Fallot	3D Slicer 4.3 (https://www.slicer.org/)	Material Extrusion
Siallagan et al	Virtual surgical planning, flow simulation, and 3-dimensional electrospinning of patient-specific grafts to optimize Fontan hemodynamics	2018	2	1–2: Fontan circulation	Mimics Innovation Suite (Materialise, Leuven, Belgium)	Material Jetting

TABLE 4.

Summary of Articles Which Were Used for Neurosurgical Planning

Authors	Title	Publication Year	n	Case Types	Processing Software	Printing Technology
Vloeberghs et al	Soft tissue rapid prototyping in neurosurgery	1998	1	1: ventricular system model	Materialise (Leuven, Belgium)	Material Extrusion
Spottiswoode et al	Preoperative three-dimensional model creation of magnetic resonance brain images as a tool to assist neurosurgical planning	2013	2	1–2: lesion in the proximity of the motor cortex	FSL (FMRIB, Oxford, UK) and MeVisLab v.2.2 (MeVis Medical Solutions AG, Bremen, Germany)	Binder Jetting
Naftulin et al	Streamlined, inexpensive 3D printing of the brain and skull	2015	7	7 skulls with 19 hemispheres and over 30 brain regions	ITK-snap (UPENN and UNC) and Blender (https://www.blender.org/)	Material Extrusion
Furdova et al	Early experiences of planning stereotactic radiosurgery using 3D printed models of eyes with uveal melanomas	2017	150	1–150: Uveal melanoma (139 choroidal melanoma, 11 ciliary body melanoma)	3D slicer (https://www.slicer.org/)	Material Extrusion
Gargiulo et al	New directions in 3D medical modeling: 3D-printing anatomy and functions in neurosurgical planning	2017	1	1: Low-grade glioma located on the frontal lobe	StealthViz (Medtronic, Minneapolis, MN) NordicBrainEx (NordicNeuroLab, Bergen, Norway), Mimics (Materialise, Leuven, Belgium)	Material Jetting
Coelho et al	Multimaterial 3D printing preoperative planning for frontoethmoidal meningoencephalocele surgery	2018	1	1: Frontoethmoidal encephalocele, nasofrontal subtype with the straigh gyrus as the content of the herniated sac	Mimics (Materialise, Leuven, Belgium)	Material Jetting
Lin et al	Using three-dimensional printing to create individualized cranial nerve models for skull base tumor surgery	2018	2	1–2: sellar region tumor, 3: acoustic neuroma	Mimics Research Version 17.0 (Materialise, Leuven, Belgium)	Material Jetting
Javan et al	Using 3D-printed mesh-like brain cortex with deep structures for planning intracranial EEG electrode placement	2020	1	1: Normal brain model (multi-material for EEG placement)	Mimics 21.0 and 3-matic 13.0 (Materialise NV, Leuven, Belgium)	Material Extrusion, Powder Bed Fusion,
Lador et al	Use of 3-dimensional printing technology in complex spine surgeries	2020	7	1–7: Complex spine oncological cases	GrabCAD (Stratasys, Rehovot, Israel)*	N/A
Ye et al	A three-dimensional color-printed system allowing complete modeling of arteriovenous malformations for surgical simulations	2020	5	1–5 Brain AVMs	Mimics (Materialise, Leuven, Belgium)	Material Jetting